ACS Pharmacology & Translational Science

Article

Cite This: ACS Pharmacol. Transl. Sci. 2018, 1, 61−72

pubs.acs.org/ptsci

DREADD Agonist 21 Is an Effective Agonist for Muscarinic-Based DREADDs *in Vitro* and *in Vivo*

Karen J. Thompson,[†] Elham Khajehali,[‡] Sophie J. Bradley,[†] Jovana S. Navarrete,[§,∥] Xi Ping Huang,[⊥] Samuel Slocum,[⊥] Jian Jin,[#] Jing Liu,[#] Yan Xiong,[#] Reid H. J. Olsen,[⊥] Jeffrey F. Diberto,[⊥] Kristen M. Boyt,[⊥] Melanie M. Pina,[⊥] Dipanwita Pati,[⊥] Colin Molloy,[†] Christoffer Bundgaard,[▽] Patrick M. Sexton,[‡] Thomas L. Kash,[⊥] Michael J. Krashes,[§,∥] Arthur Christopoulos,[‡] Bryan L. Roth,[*,⊥] and Andrew B. Tobin[*,†]

[†]Centre for Translational Pharmacology, Institute of Molecular, Cell, and Systems Biology, College of Medical, Veterinary and Life Sciences, University of Glasgow, Glasgow, Scotland G12 8QQ, United Kingdom

[‡]Drug Discovery Biology, Monash Institute of Pharmaceutical Sciences, Monash University, Parkville, Victoria 3052, Australia

[§]Diabetes, Endocrinology, and Obesity Branch, National Institutes of Diabetes and Digestive and Kidney Diseases, National Institutes of Health, Bethesda, Maryland 20892, United States

[∥]National Institute on Drug Abuse, National Institutes of Health, Baltimore, Maryland 21224, United States

[⊥]Department of Pharmacology, University of North Carolina School of Medicine, Chapel Hill, North Carolina NC2751, United States

[#]Center for Chemical Biology and Drug Discovery, Departments of Pharmacological Sciences and Oncological Sciences, Tisch Cancer Institute, Icahn School of Medicine at Mount Sinai, New York, NY10029, United States

[▽]Neuroscience, Eli Lilly & Co., Erl Wood Manor, Windlesham, Surrey GU20 6PH, United Kingdom

Supporting Information

ABSTRACT: Chemogenetic tools such as designer receptors exclusively activated by designer drugs (DREADDs) are routinely used to modulate neuronal and non-neuronal signaling and activity in a relatively noninvasive manner. The first generation of DREADDs were templated from the human muscarinic acetylcholine receptor family and are relatively insensitive to the endogenous agonist acetylcholine but instead are activated by clozapine-*N*-oxide (CNO). Despite the undisputed success of CNO as an activator of muscarinic DREADDs, it has been known for some time that CNO is subject to a low rate of metabolic conversion to clozapine, raising the need for alternative chemical actuators of muscarinic-based DREADDs. Here we show that DREADD agonist 21 (C21) (11-(1-piperazinyl)-5*H*-dibenzo[*b*,*e*][1,4]diazepine) is a potent and selective agonist at both excitatory (hM3Dq) and inhibitory (hM4Di) DREADDs and has excellent bioavailability, pharmacokinetic properties, and brain penetrability. We also show that C21-induced activation of hM3Dq and hM4Di *in vivo* can modulate bidirectional feeding in defined circuits in mice. These results indicate that C21 represents an alternative to CNO for *in vivo* studies where metabolic conversion of CNO to clozapine is a concern.

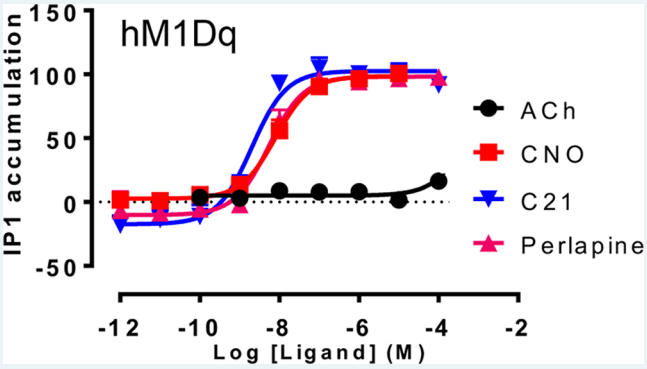

KEYWORDS: *clozapine-N-oxide, clozapine, DREADD, designer receptors exclusively activated by designer drugs, muscarinic acetylcholine receptors*

Over the past decade, several technologies have been developed to provide chemogenetic modulation of neuronal and non-neuronal signaling. These include engineered ion channels,[1,2] kinases,[3] and G protein coupled receptors (GPCRs).[4−6] Of these, it is the GPCR-based designer receptors exclusively activated by designer drugs (DREADDs)[6] that are most frequently used among neuroscientists and other biologists. Currently there are several classes of DREADDs including (1) those based on human muscarinic acetylcholine receptors (mAChRs) which are coupled to Gαq (hM1Dq and hM3Dq) and activate neuronal signaling and firing,[6,7] (2) those which are coupled to Gαi (hM4Di) and inhibit adenylate cyclase and attenuate neuronal activity and neurotransmitter release,[6] and (3) those which preferentially couple to Gαs (GsD),[8] one which preferentially couples to arrestin,[9] and one which

Received: April 30, 2018
Published: July 27, 2018

DOI: 10.1021/acsptsci.8b00012
ACS Pharmacol. Transl. Sci. 2018, 1, 61−72

activates Gαq but is not coupled to arrestin translocation.[10] Additional DREADDs based on k-opioid receptors (KORD)[11] and the free fatty acid receptor type 2 (FFAR2)[12] have also been reported. Among these, the muscarinic based DREADDs are the most commonly used and were designed to be activated by clozapine's pharmacologically inert metabolite clozapine-*N*-oxide (CNO), although as originally reported muscarinic DREADDs are also potently activated by clozapine.[6] These muscarinic DREADDs are relatively insensitive to acetylcholine[6,8] and hence can be used *in vivo* and *in vitro* to afford selective control of cellular signaling via peripheral or local administration of CNO.[7,8]

It has long been appreciated that CNO can undergo metabolic transformation to clozapine, with estimates ranging from a few percent in rodents[13] to approximately 10% in humans, nonhuman primates (NHPs) and guinea pigs.[14−16] For instance, following systemic administration of 10 mg/kg CNO, clozapine levels in cerebrospinal fluid (CSF) have been reported to reach 34 and 43 nM for the major clozapine metabolite, *N*-desmethylclozapine (NDMC).[16] Given that clozapine has potent activity at more than 50 distinct molecular targets,[17,18] while NDMC activates the M1 mAChR possibly through an atypical mechanism,[19−21] such CNO back-metabolism could give rise to the activation of a spectrum of off-target responses. Indeed, the concentrations of each CNO metabolite detected in NHP CSF are sufficient to activate off-target CNS receptors such as serotonin and dopamine receptors.[16,22]

Although the extensive literature using CNO as an effective actuator of muscarinic DREADDs (reviewed in refs 23 and 24) provides a high degree of confidence in the use of CNO: DREADD pairing and that the measurements of back metabolism of CNO could be overestimated depending upon the analytic technique used,[25] while the route of CNO administration can also affect the levels of clozapine detected post-administration.[16] It is nonetheless conceivable that even a low rate of conversion could lead to pharmacologically relevant actions of clozapine upon CNO administration.[26] Indeed, although the vast majority of published studies have not reported any measurable behavioral, cardiovascular, metabolic, or endocrinologic action of low-dose CNO in mice and rats,[26] there have been a small number of reports of actions of CNO in non-DREADD animals.[27,28] Given that both clozapine and NDMC can themselves activate both wildtype and DREADD mAChRs[19−21] and that low brain permeability for CNO has been reported,[29] it is difficult to determine whether the activation of mAChR DREADDs following CNO administration arises from CNO itself or whether this arises as a result of CNO metabolism. If CNS DREADDs are indeed activated by these metabolites, then it may be difficult to control the concentration of active drug that reaches the target site. For certain studies, therefore, where CNO back metabolism is considered to be a concern, there is a need for non-CNO chemogenetic actuators for the muscarinic DREADDs.

DREADD Agonist 21 (C21) was recently reported as a non-CNO chemogenetic actuator for muscarinic hM3Dq.[30] Meanwhile, perlapine, an approved hypnotic drug, was identified as a potential DREADD agonist during a broad library screen of existing compounds and exhibited both binding and Ca^{2+} mobilization at the hM3Dq receptor.[30] However, both compounds have only thus far been assessed at hM3Dq. Given that the M_1 and M_4 subunits are implicated in a broad range of neurodegenerative diseases and schizophrenia,[31−33] the DREADD receptors are particularly useful in dissecting signaling pathways for these subtypes. We therefore carried out a comprehensive *in vitro* and *in vivo* characterization of C21 and perlapine to assess their potential for use as an alternative to CNO. We find that C21 has (1) few off-target actions, (2) favorable pharmacokinetic properties, (3) excellent brain penetration, and (4) potently activates the hM4Di inhibitory and hM3Dq excitatory DREADDs *in vivo*. Thus, C21 represents an alternative chemogenetic actuator for studies with muscarinic-based DREADDs.

RESULTS

C21 Potently Activates hM1Dq, hM3Dq, and hM4Di *in Vitro*. We have previously reported that both C21 and perlapine potently activated hM3Dq in Chinese hamster ovary (CHO) cells transfected cells *in vitro*,[30] and their data are confirmed here with C21 and perlapine stimulating calcium mobilization at hM3Dq with a pEC_{50} of 8.48 ± 0.05 and 8.08 ± 0.05, respectively (Figure S1). We extended this analysis of C21 and perlapine to other muscarinic based DREADDs, namely, hM1Dq and hM4Dq. Using radioligand competition binding, we show that all three muscarinic DREADD ligands, CNO, C21, and perlapine, interact with the wildtype hM1 and hM4 receptors with relatively low affinity (Figure 1A,B; Table 1). Both C21 and CNO had a >10-fold higher affinity at the hM1Dq and hM4Di, whereas acetylcholine showed a >10-fold reduction in binding affinity at both muscarinic DREADD receptors (Figure 1C,D; Table 1). Unlike the other muscarinic DREADD ligands, perlapine showed only a small increase in binding affinity at hM1Dq and hM4Di compared to that of wildtype receptors (Figure 1A−D; Table 1).

In these experiments, the expression of the muscarinic receptors in transfected CHO cells were very similar between cell types (hM1 = 2 580 166 ± 185 544 sites/cell, hM1Dq = 337 998 ± 130 471, hM4 = 351 322 ± 88 571, hM4Di = 129 804 ± 15 988). Despite exhibiting modest binding affinities for wildtype hM1 receptors (Figure 1A), CNO, C21, and perlapine displayed no agonist activity in IP1 or pERK1/2 assays at this receptor (Figure 2A,B; Table 1). In contrast, all three muscarinic DREADD ligands were potent agonists in IP1 and pERK1/2 assays of hM1Dq activation (Figure 2C,D; Table 1). C21, perlapine, and CNO were also evaluated as agonists of hM4Di in assays that measure inhibition of isoproterenol-stimulated cAMP production and pERK1/2 (Figure 3A, B). At both of these responses, all three DREADD ligands had submicromolar potency at hM4Di (Figure 3A,B), whereas they had weak/no activity at the wildtype hM4 receptor (Figure 3C,D; Table 1).

Pharmacological Profile of C21. To assess the utility of C21 as a potential chemogenetic actuators suitable for *in vivo* studies, we performed a comprehensive evaluation of potential off-target activities at a large number of GPCRs via the resources of the National Institute of Mental Health Psychoactive Drug Screening Program (NIMH-PDSP). Radioligand binding studies indicated that C21 interacted with a wide range of GPCRs (Figure 4; Table S1).

To further evaluate C21 for potential off-target activity, a near genome-wide screen of C21 agonist activity at druggable nonolfactory GPCR-ome was conducted as previously described.[37] At a single concentration (5 μM), C21 showed agonist activity only at M4-, D2-, and H4-histamine receptors (Figure 5; Table S2). However, confirmatory follow-up concentration−response studies revealed minimal activity of C21 at D1-, D2-, D3-, and H4- receptors (Figure 6A−D).

DOI: 10.1021/acsptsci.8b00012
ACS Pharmacol. Transl. Sci. 2018, 1, 61−72

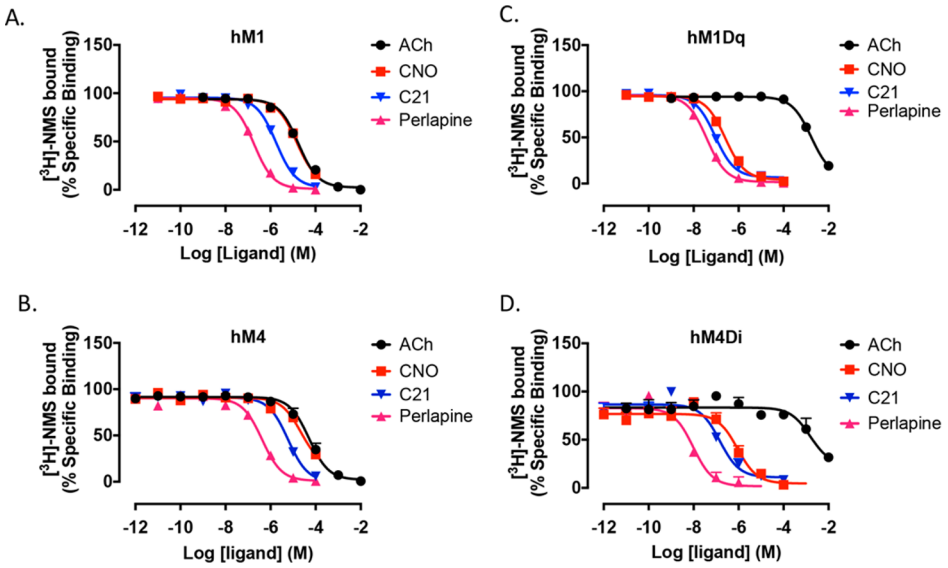

Figure 1. Binding of muscarinic DREADD ligands to DREADDs and wildtype receptors. Displacement of [^{3}H]-NMS by increasing concentrations of ACh, CNO, C21, or perlapine at (A) hM1, (B) hM4, (C) hM1Dq, and (D) hM4Di. All experiments were performed using a K_d concentration of [^{3}H]-NMS. Data represents the mean ± SEM of at least three experiments performed in duplicate.

The reason for the discrepancy between the high throughput results and the more detailed analysis is not clear, but overall our data suggests that if used *in vivo* C21 would likely show minimal off-target agonist activity at the tested 318 nonolfactory GPCRs.

Potential Antagonist Activity of C21. Given the binding data presented above indicating that C21 showed weak binding affinity to wildtype hM1 and hM4 receptors (pK_i = 5.97 and 5.44 respectively; see Table 1) as well as weak to moderate binding to a number of other nonolfactory GPCRs (see; Figure 4 and Table S1), C21 might display antagonist activity at these receptors. We therefore conducted analysis of C21 in antagonist mode at a representative group of GPCRs. At hM1 and hM4, C21 shifted the acetylcholine concentration response curve in pERK assays to the right indicating weak functional antagonism at these receptors (Figure S2a,b). We also observed antagonism of C21 at human D1 receptors using a cAMP assay and human D2 receptors using a G_i-dissociation assay (Figure S3a,b). In the case of human H4 histamine receptors which bound C21 with very low affinity (pK_i < 5, Table S1) no antagonism was observed in a G_i-dissociation assay (Figure S3c).

These data indicated that although C21 was a highly selective and potent agonist for muscarinic DREADDs (pEC_{50} for hM1Dq = 8.91 and that for hM4Di = 7.77) the fact that C21 showed weak to moderate binding affinity at a range of wildtype GPCRs (including wildtype muscarinic receptors) it is possible that this might translate to functional antagonism *in vivo*. As such, care needs to be taken with *in vivo* dosing of C21 to ensure that the free concentration of compound remains in a range that activates muscarinic DREADDs but is sufficiently low to avoid antagonism at wildtype GPCRs.

Pharmacokinetic Properties of C21 and Perlapine. The *in vitro* analysis of C21 encouraged further evaluation of this compound as an alternative *in vivo* chemogenetic actuator by analysis of the pharmacokinetic properties of C21 compared to CNO and perlapine. Intraperitoneal administration of CNO at 0.3, 1, and 1.5 mg/kg led to elevations in plasma levels of the compound, but there was no evidence of CNO in the brain (Figure 7A). Since CNO can be back-metabolized to clozapine, the concentrations of clozapine following CNO administration were also determined. Clozapine was present in both the plasma and brain, at levels indicative of significant back-metabolism of CNO in these animals (Figure 7A). It is noteworthy that clozapine in these brain samples displayed 95% protein binding. In contrast to CNO, intraperitoneal (i.p.) administration of both C21 and perlapine at 0.1, 1, and 10 mg/kg demonstrated measurable brain and plasma levels of each compound 30 min after administration with no evidence of metabolism to clozapine (Figure 7B,C). A time course of C21 accumulation in the brain and plasma following administration of 5 mg/kg demonstrated that plasma levels peaked at 1150 ng/mL (4.12 μM), whereas brain levels reached 579 ng/mL (2 μM) (Figure 7D). Despite these relatively high concentrations, C21 displayed 95.1% plasma protein binding (4.7% unbound) and 95% brain protein bounding (4.9% unbound) (Figure 7E). Thus, the effective free concentrations of C21 at the peak measured in these studies represent ~54 nM in plasma and 28 nM brain. On the basis of these pharmacokinetic considerations, we opted to evaluate C21 in mice at doses as low as 0.3 mg/kg which were calculated to afford a free brain concentration of C21 of ~1.7 nM. Additionally, we chose not to exceed doses of 3 mg/kg, which would achieve a free concentration of ~17 nM, to minimize potential off-target actions.

C21 Activates Neuronal hM3Dq *in Vitro* and *in Vivo*. The studies described above together with our previous work using hM3Dq[30] support the notion that C21 is a potential alternative actuator of muscarinic-based DREADDs *in vivo*. To test this notion further, we focused on hM3Dq, a muscarinic DREADD commonly used by neurobiologists to activate neuronal circuitary. Our initial studies were performed with lateral hypothalamic vGAT-expressing neurons virally induced to express hM3Dq. In these preparations, C21 (1 μM) was seen to cause depolarization in hM3Dq-expressing neurons but not in control infected neurons (Figure 8A,B). As activation of these neurons *in vivo* by peripheral CNO administration has been previously demonstrated, we next tested a cohort of mice with increasing doses of C21. As can be seen, C21 drives feeding in

DOI: 10.1021/acsptsci.8b00012
ACS Pharmacol. Transl. Sci. 2018, 1, 61−72

Table 1. Comparative Binding and Activity Properties of Muscarinic DREADD Ligands[a]

	hM1			hM$1D_q$			hM4			hM4Di		
	pK_i	pEC_{50} IP_1	pEC_{50} pERK	pK_i	pEC_{50} IP_1	pEC_{50} pERK	pK_i	pEC_{50} pERK	pEC_{50} cAMP	pK_i	pEC_{50} pERK	pEC_{50} cAMP
ACh	4.96 (±0.09) $N = 9$	7.59 (±0.16) $N = 9$	5.76 (±0.16) $N = 12$	2.83 (±0.07) $N = 8$	3.09 (±0.27) $N = 8$	2.45 (±0.18) $N = 7$	4.82 (±0.15) $N = 3$	7.51 (±0.30) $N = 6$	6.92 (±0.13) $N = 4$	2.66 (±0.11) $N = 3$	2.73 (±0.28) $N = 3$	2.75 (±0.09) $N = 4$
CNO	5.10 (±0.03) $N = 7$	N/A	N/A	6.74 (±0.10) $N = 9$	8.61 (±0.03) $N = 10$	7.70 (±0.25) $N = 11$	4.85 (±0.05) $N = 3$	N/A	4.82 (0.43) $N = 3$	6.30 (±0.22) $N = 3$	6.89 (±0.12) $N = 3$	7.29 (±016) $N = 4$
C21	5.97 (±0.05) $N = 7$	N/A	N/A	7.20 (±0.21) $N = 8$	8.91 (±0.01) $N = 4$	6.54 (±0.52) $N = 3$	5.44 (±0.11) $N = 3$	N/A	5.73 (±0.13) $N = 3$	6.75 (±0.26) $N = 3$	7.77 (±0.31) $N = 3$	7.75 (±0.14) $N = 4$
perlapine	7.04 (±0.06) $N = 7$	N/A	N/A	7.58 (±0.07) $N = 8$	8.38 (±0.07) $N = 7$	6.80 (±0.19) $N = 4$	6.58 (±0.10) $N = 3$	N/A	7.25 (±0.71) $N = 3$	7.17 (±0.08) $N = 3$	7.27 (±0.33) $N = 3$	7.20 (±0.19) $N = 4$

[a]Summary for the binding affinities (pK_i) and potency (pEC_{50}) for ACh and CNO at various signal transduction assays of C21 and perlapine at muscarinic DREADDs and wildtype receptors. Data represents the mean ± SEM of at least three independent experiments carried out in duplicate.

a dose-dependent fashion (Figure 8C−E) with a maximal response similar to 3 mg/kg CNO (Figure 8F).

Agouti-related peptide (AgRP) neurons, localized in the arcuate nucleus (ARC), display appetite-state-dependent, dynamic activity changes[38−41] and are critical regulators of appetite.[42−45] Acute chemogenetic activation of ARC^{AgRP} neurons utilizing stimulatory G_q-coupled DREADDs and the ligand CNO rapidly and robustly escalates feeding behavior in calorically replete mice.[42,46] Here, we assessed the capacity of C21 to activate hM3Dq expressed in ARC^{AgRP} neurons and evoke food intake in sated animals. We found that C21-mediated stimulation of AgRP-hM3Dq-expressing ARC^{AgRP} neurons dose-dependently promoted food consumption at comparable levels to CNO administered at the same concentrations (Figure 9A−C). Importantly, neither C21 nor CNO affected feeding behavior in wildtype, (non-Cre-expressing) littermate controls injected with AAV-DIO-hM3Dq-mCherry (Figure 9D−F).

C21 Drives Behaviors Modulated by hM4Di *in Vivo*. The paraventricular nucleus (PVH) is a key anatomical structure for the maintenance of energy balance and has recently been identified as a downstream signaling site of ARC^{AgRP} neurons.[38,47,48] Single-minded 1 (SIM1) is a transcription factor necessary for proper development of the PVH. Conditional, postnatal *SIM1* knockout mice as well as animals devoid of PVH^{SIM1}-expressing neurons display hyperphagia-induced obesity.[49,50] Additionally, chemogenetic silencing of PVH^{SIM1} neurons promptly drives food consumption in otherwise sated mice.[47,51] Here, we examined the sufficiency of C21 to activate hM4Di expressed in PVH^{SIM1} neurons and facilitate food intake in calorically replete mice. We found that C21-mediated stimulation of hM4Di-expressing PVH^{SIM1} neurons substantially enhanced food consumption at comparable levels to CNO administered at the same concentrations (Figure 10 A,B). Notably, as observed in wildtype, neither C21 nor CNO ligand influenced food intake in a separate cohort of wildtype, (non-Cre-expressing) littermate control mice injected with AAV-DIO-hM4Di-mCherry (Figure 10C,D).

DISCUSSION

Muscarinic receptor based DREADDs activated by CNO have proven powerful tools to determine signaling pathways that underlie central and peripheral responses.[23,24] The majority of these previous *in vivo* studies have been conducted with CNO doses that were sufficient to show a response only in the DREADD expressing animals and not in control animals. Under these carefully controlled conditions the responses observed following CNO administration can only have been derived from activation of DREADD receptors. Hence, provided rigorous experimental design is employed, using CNO as an actuator of the muscarinic DREADDs has proven to be a perfectly valid approach.

Despite the success of CNO:DREADD pairing the back metabolism of CNO to clozapine as demonstrated in both rodent and nonhuman primates[13−15] have raised concerns that clozapine and not CNO might be the activator of genetically engineered DREADD receptors in animal studies.[28] In support of these concerns are the data presented here where we were unable to detect CNO in the brain following intraperitoneal administration of CNO; rather, clozapine was detected in the brain and increased in a dose-dependent manner following CNO administration. Importantly, the levels of clozapine achieved following CNO administration was not sufficient to

DOI: 10.1021/acsptsci.8b00012
ACS Pharmacol. Transl. Sci. 2018, 1, 61−72

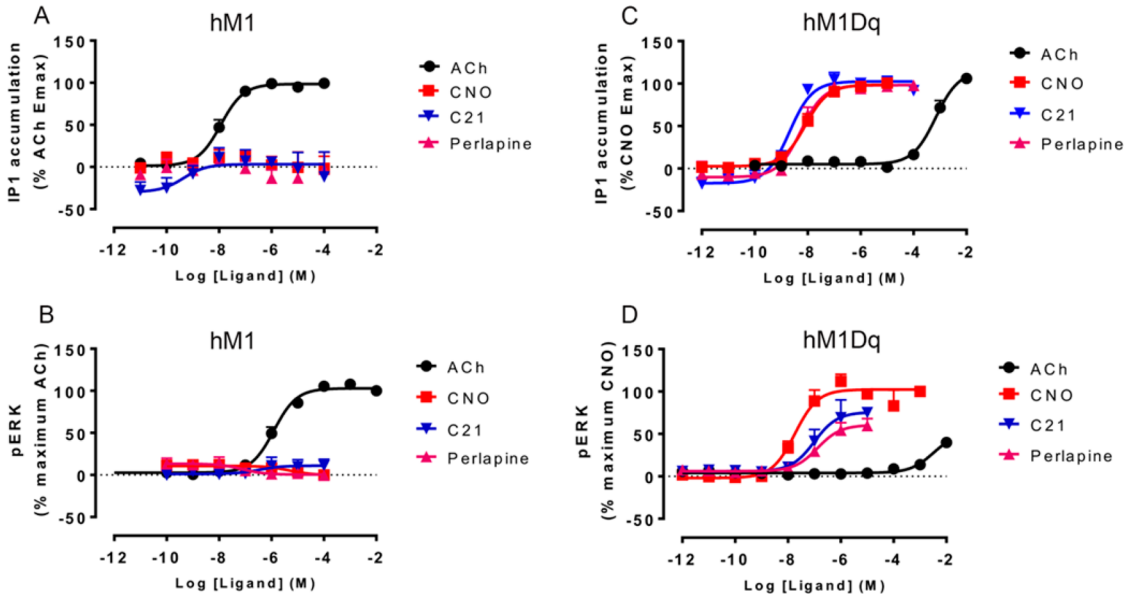

Figure 2. Signaling at hM1 and hM1Dq mediated by muscarinic DREADD ligands. Concentration response curves for ACh, CNO, C21, and perlapine in (A) IP_1 accumulation mediated by hM1, (B) ERK 1/2 activation mediated by hM1, (C) IP_1 accumulation mediated by hM1Dq, and (D) ERK 1/2 activation mediated by hM1Dq. Data represents the mean ± SEM of at least three experiments performed in duplicate.

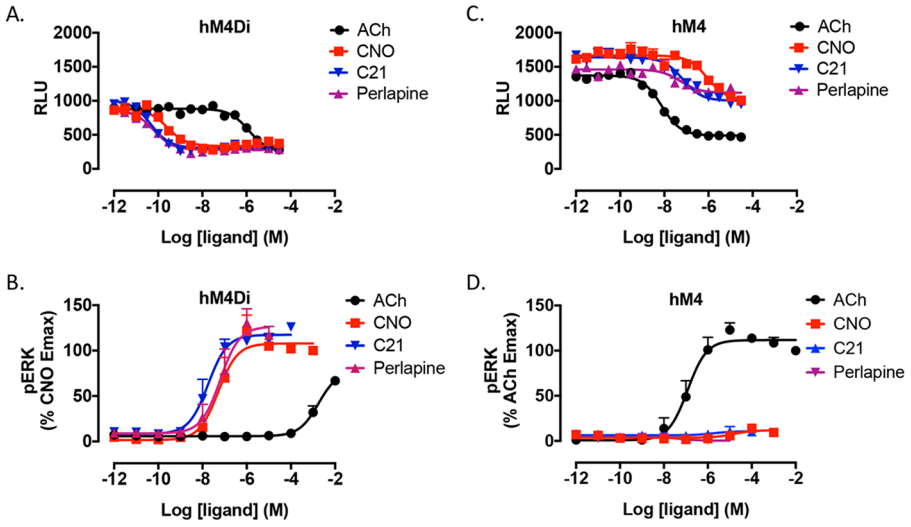

Figure 3. Signaling at hM4 and hM4Di mediated by muscarinic DREADD ligands. Concentration response curves for ACh, CNO, C21, and perlapine in (A) inhibition of isoproterenol elevated cAMP by hM4Di, (B) ERK 1/2 activation mediated by hM4Di, (C) inhibition of isoproterenol elevated cAMP by hM4, and (D) ERK 1/2 activation mediated by hM4. Data represents the mean ± SEM of at least three experiments performed in duplicate.

induce off-target effects in wildtype animals (for example on feeding behavior) even at supra-maximal doses (e.g., 3 mg/kg). Hence, in our hands, as seen in many other studies (e.g., refs 42, 52, and 53), effects of CNO administration on behavior was only evident in mice induced to express muscarinic DREADDs. Thus, the levels of CNO back metabolism observed here were not sufficient to mediate significant changes for the observed responses in animals not expressing muscarinic DREADDs.

To address the concerns regarding back-metabolism of CNO, we set out to establish if novel DREADD ligands, based on the CNO scaffold, might offer an alternative actuator of muscarinic DREADDs. Here we investigated two such ligands, C21 and perlapine, which we have previously shown to act as agonists at the G_q DREADD, hM3Dq,[30] and which we report do not undergo back-metabolism to clozapine. While both of these ligands interacted with the wildtype hM1 and hM4 receptors, they showed >10-fold higher affinity for the DREADD variants of these receptors and importantly act as agonists at hM1Dq and hM4Di while lacking agonist activity at wildtype receptors. Against a panel of nonolfactory GPCRs, C21 and perlapine showed at least 10-fold lower affinity for the majority of GPCRs tested than seen for the muscarinic DREADDs. There were however some exceptions, such as members of the serotonin receptor family (e.g., 5HT2A, 5HT2C, and 5HT7) as well as the dopamine D1 and histamine H1 receptors, where affinities for both C21 and perlapine were similar to, or greater than, that observed for the muscarinic DREADDs. Despite these data demonstrating binding of C21 to some GPCR targets, activity assays conducted on a panel of 318 nonolfactory GPCRs, and subsequent confirmatory

DOI: 10.1021/acsptsci.8b00012
ACS Pharmacol. Transl. Sci. 2018, 1, 61−72

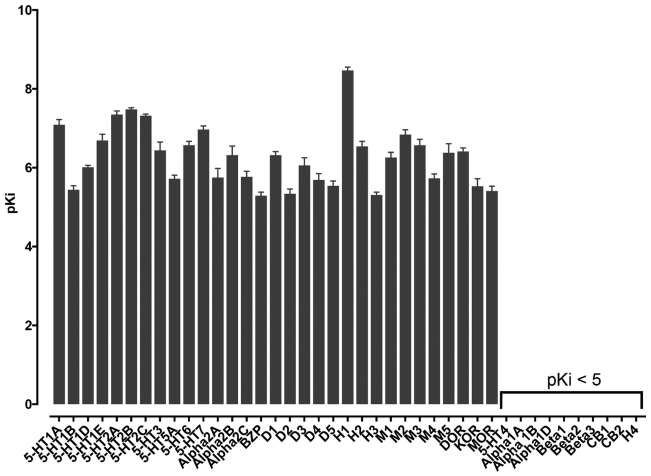

Figure 4. Determination of C21 and perlapine binding affinities at a panel of GPCR drug targets. Binding affinity (pK_i) was determined at indicated receptors and targets using radioligand binding assays with membrane preparations and provided by NIMH PDSP. Results were presented as mean ± SEM from a minimum of 3 independent assays, each in triplicate. Indicated are those receptors where the pK_i values are less than 5. The raw data is presented in Table S1.

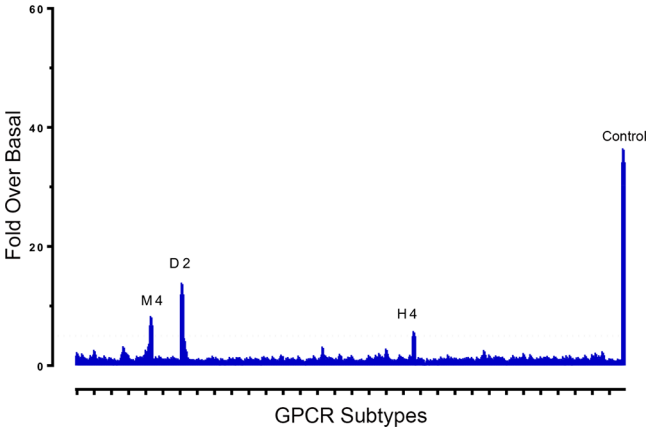

Figure 5. Assessment of off-target activity of C21 against 318 nonolfactory GPCR targets. Agonist activity of C21 at 318 nonolfactory human GPCRs at a final of 5 μM. Results were represented as fold of basal in quadruplicate. Dopamine receptor DRD2 with 100 nM Quinpirole served as an assay control (Control). The GPCRome screening assay was carried out as outlined in the Methods section and plotted using Prism. The raw data is presented in Table S2.

studies, indicated that C21 was devoid of activity at the receptors tested, including receptors of the dopamine, serotonin, and histamine receptor families. Hence, C21 appeared to be a highly selective muscarinic DREADD actuator with no evidence of significant off-target GPCR agonist activity.

There does however remain the possibility that C21 might act as a functional antagonist at those GPCRs to which binding was observed. We tested this possibility directly for a subset of wildtype GPCRs and determined that at least in the case of the wildtype hM1, hM4, hD1, and hD2 receptors that C21 did indeed act as a weak antagonist. It is therefore important for researchers using C21 *in vivo* to bear in mind that high doses of C21 might lead to levels of free ligand that mediate GPCR antagonism. *In vivo* experiments must therefore be conducted with the appropriate controls where C21 is administered to animals that do not express the muscarinic DREADDs. In this

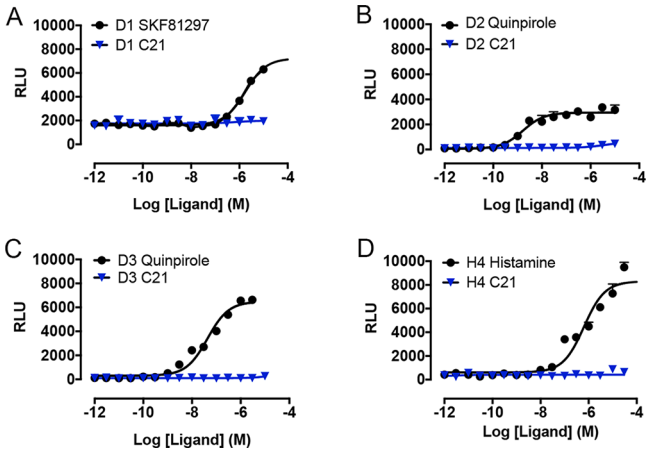

Figure 6. Assessment of activity of C21 at dopamine D1−D3 and histamine H4 receptors. Activation of cAMP signaling at (A) dopamine D1 receptors stimulated with C21 and SKF81297, (B) dopamine D2 receptors stimulated with C21 and quinpirole, (C) dopamine D3 receptors stimulated with C21 and quinpirole, and (D) histamine H4 receptors stimulated with C21 and histamine. Data shown represents the mean ± SEM of at least three independent experiments performed in duplicate.

way, off-target C21 behaviors/responses will be clearly identified. In the *in vivo* experiments conducted in our study, we found that concentrations of C21 that resulted in changes in feeding behavior in the muscarinic DREADD expressing animals had no off-target effects in control animals where muscarinic DREADDs were not expressed (see discussion below).

The *in vivo* activity of C21 was tested by viral-induced expression of hM3Dq in LH^{vGAT} or ARC_{AgRP} neurons of the hypothalamus which have previously been shown to induce feeding on CNO administration.[46,54] Employing this model, C21 administered at doses that gave no feeding response in animals expressing wildtype hM3 produced a robust feeding response that mimicked that seen with CNO. Similarly, silencing of SIM1 neurons in the paraventricular hypothalamus via activation of virally transduced hM4Di has previously been associated with an increase in feeding response.[52] Here administration of C21 mimicked CNO activity by increasing feeding in this model. Collectively, these *in vivo* studies support the notion that C21 represents an effective alternative actuator for muscarinic DREADDs.

Overall, we conclude that whereas CNO has proved to be an effective actuator of muscarinic DREADDs and, provided controls are in place, will continue to be an excellent ligand tool, concerns regarding potential off-target responses arising from back-metabolism of CNO to clozapine might be overcome by using C21 as an alternative selective agonist for muscarinic DREADDs.

METHODS

Mouse Handling for Feeding Studies. Animal care procedures were approved at the National Institutes of Health as well as UNC and the UK Home Office. Mice (10−12 week old males) were singly housed for at least 2.5 weeks following surgery and handled for 10 consecutive days before the assay to reduce stress response. Feeding studies were performed in home cages with ad libitum food access. Home cages were changed every day during food intake measurements to eliminate residual food crumbs in the bedding. CNO or C21 was administered at

DOI: 10.1021/acsptsci.8b00012
ACS Pharmacol. Transl. Sci. 2018, 1, 61−72

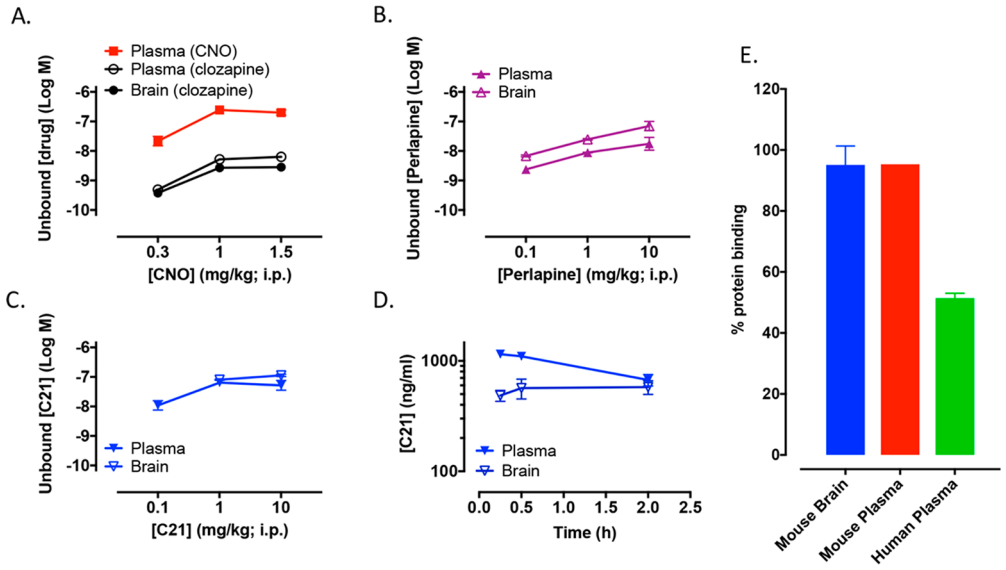

Figure 7. Analysis of brain and plasma exposure for CNO, C21, and perlapine. (A) Unbound fraction of plasma and brain CNO and clozapine levels following i.p. administration of various concentrations of CNO. (B) Unbound fraction of plasma and brain levels of perlapine following i.p. administration of various concentrations of perlapine. (C) Unbound fraction of plasma and brain levels of C21 following i.p. administration of various concentrations of C21. (D) Time course of C21 brain and plasma exposure following i.p. administration of C21 (5 mg/kg). (E) Percentage protein binding of C21 in human and mouse plasma and mouse brain homogenate. Data shown represents the mean ± SEM of at least three independent experiments.

0.3, 1.0, or 3.0 mg per kg of body weight. Saline was delivered at the same volume as CNO or C21 to maintain consistency in the studies. Mice with "missed" viral injections, incomplete "hits", or expression outside the area of interest were excluded from analysis after post hoc examination of mCherry expression.

Feeding Studies in *Sim1-Cre* Mice. During the light cycle, animals injected with AAV8-hSyn-DIO-hM4Di-mCherry (*Sim1-Cre*, $n = 6$; WT, $n = 6$) were injected with either saline, CNO, or C21 (i.p.) and food intake was measured 0.5, 1.0, 2.0, and 3.0 h after injection. A full trial consisted of assessing food intake from the study subjects after they received injections of saline, CNO, and C21 over 3 days in a crossover design.

Feeding Studies in *Agrp-ires-Cre* Mice. During the light cycle, animals injected with AAV8-hSyn-DIO-hM3Dq-mCherry (*Agrp-ires-Cre*, $n = 6$; WT, $n = 4$) were injected with either saline, CNO, or C21 (i.p.), and food intake was measured 0.5, 1.0, 2.0, and 3.0 h after injection. A full trial consisted of assessing food intake from the study subjects after they received injections of saline, CNO, and C21 over 3 days in a crossover design.

Whole-Cell Radioligand Binding Assays. FlpIn CHO cells stably expressing the hemaglutinine (HA)-tagged wildtype human M1 or M4 (hM1 or M4 WT) mAChRs were plated at the density of 20 000, and the human M1 DREADD (hM1Dq) or M4 DREADD (hM4Di) mAChRs were plated at 50 000 cells per well of 96-well white clear-bottomed Isoplates (PerkinElmer Life Sciences, Boston, MA), and grown overnight.

Saturation binding assays were performed to estimate the expression levels (B_{max}) and equilibrium dissociation constant of the radioligand (K_d). Cells were washed twice with phosphate-buffered saline (PBS), and incubated with 0.03–10 nM [^{3}H]NMS in a final volume of 100 μL of buffer (20 mM HEPES, 100 mM NaCl, 10 mM $MgCl_2$, pH 7.4) for 4 h at room temperature. Atropine at the final concentration of 100 μM was used to determine nonspecific binding.

For equilibrium binding assays, cells were incubated with increasing concentrations of the ligands or 100 μM atropine, for nonspecific binding, in the presence of K_d concentration of the radioligand for 4 h at room temperature. The assays were terminated by rapid removal of the radioligand, and two washes with 100 μL/well ice-cold 0.9% NaCl buffer. Radioactivity was determined by addition of 100 μL/well MicroScint scintillation liquid (PerkinElmer Life Sciences, Boston, MA) and counted on a MicroBeta plate reader (PerkinElmer Life Sciences, Boston, MA).

IP-One Accumulation Assays. FlpIn CHO-hM1 WT, hM4 WT, hM1Dq, or hM4Di cells were seeded at the density of 10 000 per well in 96-well transparent cell culture plates. The following day, cells were preincubated for 1 h with IP_1 stimulation buffer (1 mM $CaCl_2$, 0.5 mM $MgCl_2$, 4.2 mM KCl, 146 mM NaCl, 5.5 mM D-glucose, 10 mM HEPES, and 50 mM LiCl, pH 7.4). Cells were then stimulated with ligands in IP_1 stimulation buffer for 1 h at 37 °C, 5% CO_2, and then lysed with 40 μL/well (for hM1 or M4 WT) or 25 μL/well (for hDi or Dq) IP_1 lysis buffer (50 mM HEPES pH 7.0, 15 mM KF, 1.5% v/v Triton-X-100, 3% v/v FBS, 0.2% w/v BSA). IP_1 levels were measured by incubation of cell lysates with FRET reagents (the cryptate-labeled anti-IP1 antibody and the d2-labeled IP1 analogue) for 1 h at 37 °C. The emission signals were measured at 590 and 665 nm after excitation at 340 nm on an EnVision plate reader (PerkinElmer Life Sciences, Boston, MA). Signals were expressed as the FRET ratio $F = (\text{fluorescence}_{665nm}/\text{fluorescence}_{590nm}) \times 10^4$ and normalized to the maximal response to ACh (for hM1 WT or hM4 WT) or CNO (for hM1Dq or hM4Di).

ERK1/2 Phosphorylation (pERK1/2) Assays. FlpIn CHO-hM1 WT, hM4 WT, hM1Dq, or hM4Di cells were at seeded at 10 000 cells per well in 96-well transparent cell culture plates. The following day, cells were washed twice with PBS and incubated in serum-free DMEM, supplemented with 8 mM HEPES for 6 h at 37 °C to reduce FBS-stimulated

DOI: 10.1021/acsptsci.8b00012
ACS Pharmacol. Transl. Sci. 2018, 1, 61–72

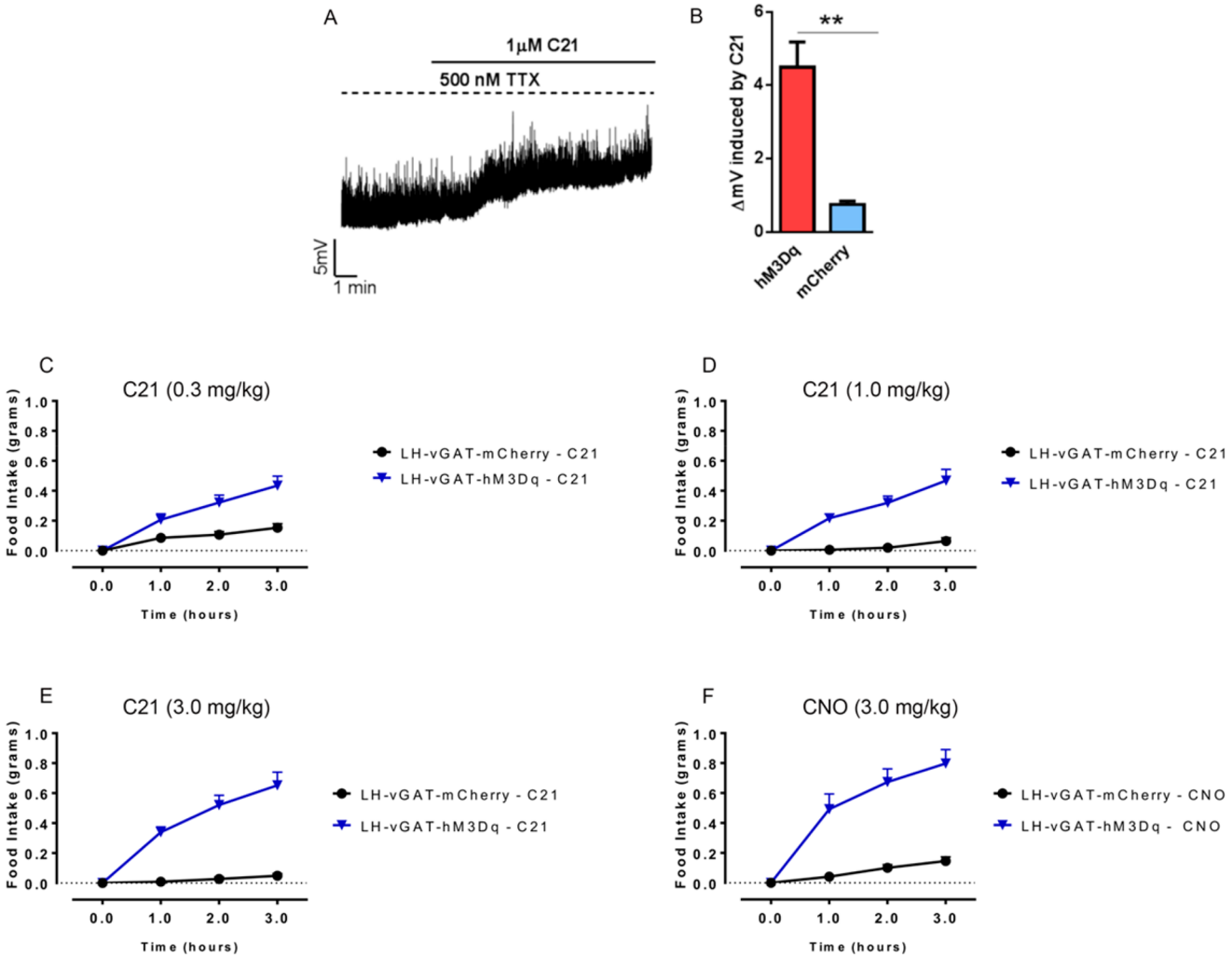

Figure 8. C21 and CNO activates hM3Dq in neuronal cultures and *in vivo*. Recordings from lateral hypothalamic vGAT neurons infected with AAV encoding either hM3Dq-mCherry or mCherry. Neurons were exposed to C21 (1 μM) in the presence of tetrodotoxin (TTX, 500 nM). (A) Representative trace and (B) histogram on the right is the mean ± SEM with n = 6 cells for the hM3Dq and n = 3 cells for the mCherry (* indicates $p < 0.05$, Student's t test). (C–F) Food intake in animals in which hM3Dq or mCherry was virally induced to be expressed in LH-vGAT neurons followed by administration of (C) C21 (0.3 mg/kg) (D) C21 (1.0 mg/kg), (E) C21 (3.0 mg/kg), and (F) CNO (3.0 mg/kg). Data represents the mean ± SEM of 11 mCherry mice and 10 hM3Dq mice.

pERK1/2 levels. In all experiments, 10% FBS was used as a positive control to measure the maximal levels of pERK1/2 stimulation. Time course experiments were first performed to determine the time at which the maximal pERK1/2 signal is produced in response to each ligand (ACh at 100 μM and all other ligands at 10 μM) over a 20 min period (0, 2, 5, 7, 10, 15, and 20 min) at 37 °C.

Concentration–response curves were generated by incubation of cells with increasing concentrations of each ligand for 5 min at 37 °C, as determined in the time course assays. Assays were terminated by the removal of drugs and lysing the cells with 50 μL/well SureFire lysis buffer (PerkinElmer Life Sciences, Boston, MA). Following agitation for 10–15 min, 5 μL of cell lysates were transferred into a 384-well white opaque Proxiplate (PerkinElmer Life Sciences, Boston, MA), and incubated with 8 μL of a mixture of reaction buffer, activation buffer, acceptor beads, and donor beads in a ratio of 6:1:0.3:0.3 for 1.5 h in the dark at 37 °C. The signals were measured on an EnVision plate reader (PerkinElmer Life Sciences, Boston, MA) and normalized to the maximal response to ACh (for hM1 WT or hM4 WT) or CNO (for hM1Dq or hM4Di).

Radioligand Binding Assays with Membranes. Radioligand binding assays with membrane preparations to determine binding affinity were carried out as outlined before[55] and by the National Institute of Mental Health's Psychoactive Drug Screening Program (NIMH PDSP) (https://pdsp.unc.edu/), Contract # HHSN-271–2013–00017-C. The NIMH PDSP is Directed by B.L.R. at the University of North Carolina at Chapel Hill, Chapel Hill, NC, and Project Officer Jamie Driscoll at NIMH, Bethesda, MD.

G_i-Mediated cAMP Production (GloSensor cAMP) Assays. HEK293 T cells were used for transient transfections and G_i mediated cAMP production assays. Assays were performed according to published procedures (PMID25895059, PRESTO-Tango paper). More detailed assay protocols are available at NIMH PDSP Web site (http://pdspdb.unc.edu/pdspWeb/?site=assays).

G_q-Mediated Calcium Release (FLIPR) Assays. CHO cells stably expressing human $M3D_q$ receptors were used for G_q-mediated calcium release assays. Assays were performed according to published procedures (PMID25895059, PRESTO-Tango paper). More detailed assay protocols are available

DOI: 10.1021/acsptsci.8b00012
ACS Pharmacol. Transl. Sci. 2018, 1, 61–72

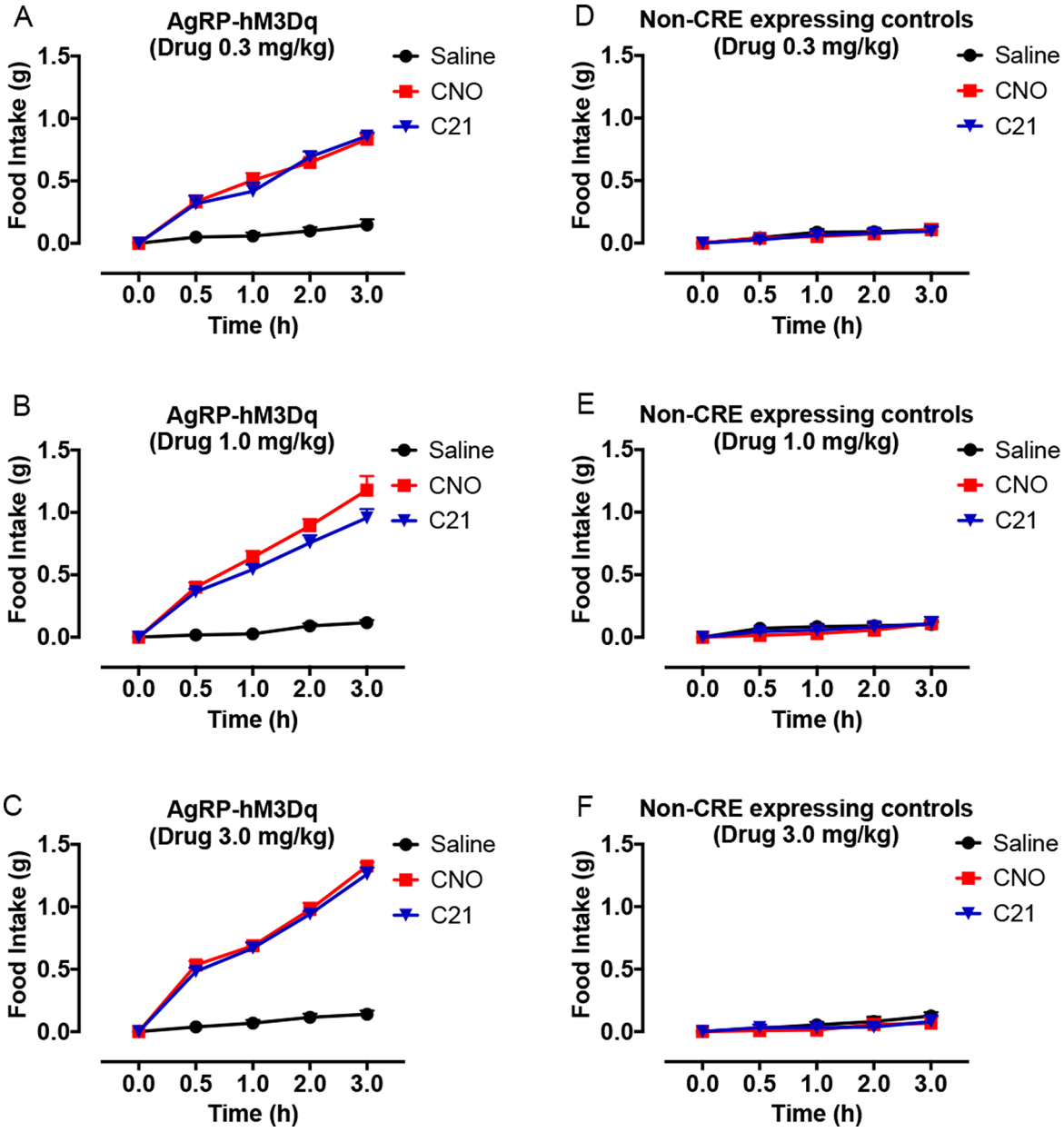

Figure 9. *In vivo* activation of hM3Dq expressed in ARC^{AgRP}-neurons by C21 and CNO increases feeding behavior in sated mice. Light cycle food intake was monitored following CNO or C21 administration at various concentrations to calorically replete AgRP-ires-CRE-expressing animals infected with (A–C (n = 6)) AAV-DIO-hM3Dq-mCherry or (D–F (n = 6)) control non-CRE-expressing animals infected with AAV-DIO-hM3Dq-mCherry. Data represents the mean ± SEM.

at NIMH PDSP Web site (http://pdspdb.unc.edu/pdspWeb/?site=assays).

GPCRome Screening (PRESTO-Tango) Assays. Potential agonist activity at human GPCRome was measured using the PRESTO-Tango assay as published (PMID25895059, PRESTO-Tango paper) with modifications. Briefly, HTLA cells were plated in 384-well white plates overnight and transfected with receptor tango constructs (15 ng/well) for 24 h. Transfected cells were then incubated with compounds in DMEM supplemented with 1% dialyzed FBS for 18 h. Medium and compound mixture were removed, and BrightGlo reagents (Promega) were added to determine luciferase reporter activity. The assay was designed so that each receptor construct had 4 replicate wells for testing drug and 4 replicate wells for medium (vehicle) control. Results were represented in the form of fold over average basal (vehicle control) for each receptor. Dopamine receptor DRD2 is used as an assay control with 100 nM Quinpirole in each assay plate. Most receptors showed activity from 0.5- to 2.0-fold of basal level. Follow-up assays are usually not planned for observed activity with less than 3.0-fold of basal level.

G_{i1} BRET Dissociation Assay. Separate pcDNA plasmids containing the sequence for Gβ_1, Gγ_2-GFP^2, G$_{i1}$-Rluc8, and either human dopamine D2 receptor or histamine H4 receptor were cotransfected into HEK293T cells (in 10 cm plates) at 1.5 μg/construct using Transit-2020 (Mirus) at a ratio of 3 μL/μg Transit/DNA. The next day, cells were harvested and plated in DMEM containing 1% dFBS in polylysine-coated 96-well plates (Greiner) at 50 000 cells per well. Sixteen hours later, media was aspirated from each well, and cells were

DOI: 10.1021/acsptsci.8b00012
ACS Pharmacol. Transl. Sci. 2018, 1, 61–72

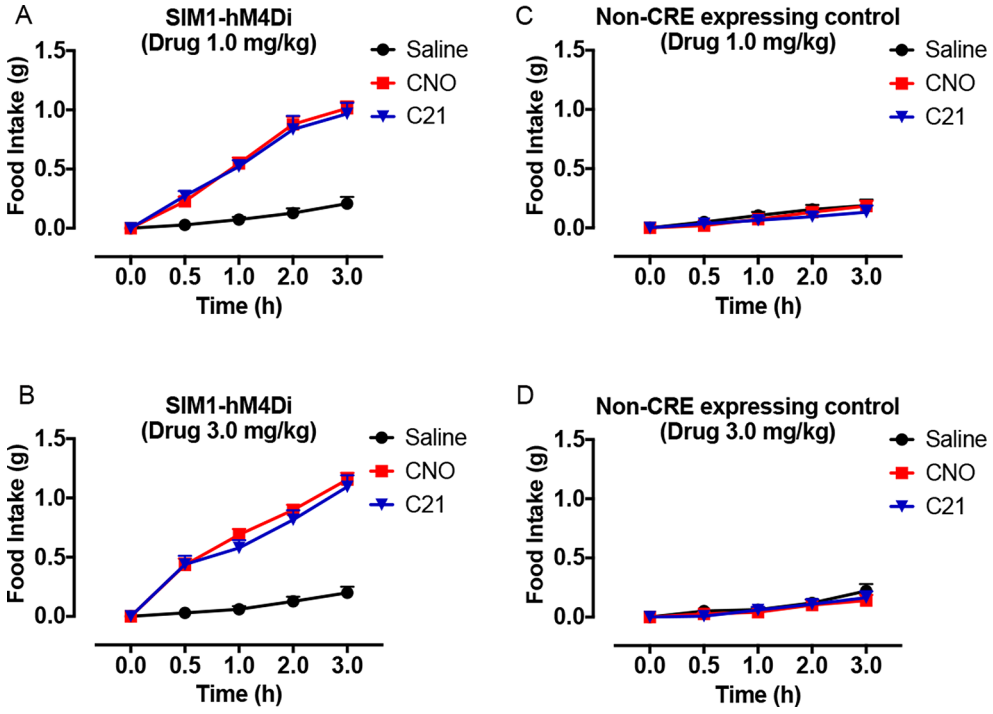

Figure 10. *In vivo* activation of hM4Di expressed in PVH^{SIM1}-neurons by C21 and CNO increases feeding behavior in sated mice. Light cycle food intake was monitored following CNO or C21 administration at various concentrations to calorically replete SIM1-CRE-expressing animals infected with (A, B (n = 6)) AAV-DIO-hM4Di-mCherry or (C, D (n = 6)) control non-CRE-expressing animals infected with AAV-DIO-hM4-mCherry. Data represents the mean ± SEM.

subsequently rinsed with 60 μL of assay buffer (20 mM HEPES, 1× Hanks Buffered Saline Solution, pH 7.4). Before drug treatment, 60 μL of fresh assay buffer was added to each well followed by 10 μL of 50 uM Coelenterazine 400a (Prolume). Luminescence and fluorescence were measured using an LB940 Mithras (Berthold technologies), and BRET was computed as the ratio of GFP^2 fluorescence to luciferase signal.

cAMP Glo-sensor. HEK293T cells in 10 cm plates were transfected with 4 μg of Glosensor and 4 μg of DNA encoding the human dopamine D1 receptor. The next day, cells were harvested and plated in polylysine-coated 384-well plates (Greiner) at a density of 20 000 cells/well in DMEM containing 1% dFBS. The next day, media was aspirated from each well and replaced with 20 μL of assay buffer containing 4 mM luciferin. Then, 10 μL of drugs were added 30 min later, and plates were read after 15 min.

Data Analysis. All data were analyzed using GraphPad Prism 7 (San Diego, CA). [^{3}H]NMS inhibition binding data were analyzed according to a one-site binding model,[34] and the equilibrium dissociation constants (K_i) of unlabeled ligands were calculated using the Cheng and Prusoff equation[35] by constraining the radioligand K_d to the values estimated from saturation binding assays. Concentration−response curves generated from IP_1 or pERK1/2 assays were fitted to a three-parameter logistic equation. All affinity and potency values were estimated as logarithms.[36]

Schild Analysis. For acetylcholine, dopamine or histamine concentration response curves (Figures 2 and 3) in the presence of multiple concentrations of C21 the following form of the Gaddum and Schild equations was applied globally to the data sets:

$$Y = \text{Bottom} + \frac{(\text{Top} - \text{Bottom})}{1 + \left(\frac{10^{\log EC_{50}\left(1+\frac{[B]}{10^{-pA_2}}\right)^s}}{[A]} \right)^{n_H}}$$

where "Top" represents the maximal asymptote of the curves, "Bottom" represents the minimum asymptote of the curves, log EC_{50} represents the logarithm of the agonist EC_{50} in the absence of C21, [A] represents the concentration of agonist, [B] represents the concentration of C21, n_H represents the Hill slope of the agonist curve, s represents the Schild slope for C21, and pA_2 represents the negative logarithm of the concentration of C21 that shifts the agonist EC_{50} by a factor of 2. In the absence of C21 ([B] = 0), this equation becomes the standard four-parameter logistic equation for fitting agonist concentration−response data.

■ ASSOCIATED CONTENT

Supporting Information

The Supporting Information is available free of charge on the ACS Publications website at DOI: 10.1021/acsptsci.8b00012.

Measurement of muscarinic DREADD receptor responses, effects of DREADD ligands at muscarinic receptor, dopamine and histamine receptors and binding and activity of muscarinic DREADD ligands on a panel of GPCRs (PDF)

Receptor pK_i data (XLSX)

Receptor versus fold over basal (XLSX)

■ AUTHOR INFORMATION

Corresponding Authors

*E-mail: bryan_roth@med.unc.edu.

*E-mail: Andrew.tobin@glasgow.ac.uk.

DOI: 10.1021/acsptsci.8b00012
ACS Pharmacol. Transl. Sci. 2018, 1, 61−72

ORCID

Jian Jin: 0000-0002-2387-3862
Patrick M. Sexton: 0000-0001-8902-2473
Andrew B. Tobin: 0000-0002-1807-3123

Author Contributions

K.J.T. and E.K. contributed equally to this work.

Author Contributions

A.B.T. and B.L.R. wrote the paper. A.B.T., B.L.R., and A.C. conceived the project. A.B.T., B.L.R., A.C., P.M.S., S.J.B., T.L.K., and M.J.K. lead experimental design and analyzed data. K.J.T., E.K., J.S.N., X.P.H., S.S., J.J., J.L., Y.X., R.H.J.O., J.F.D., K.M.B., M.M.P., D.P., C.M., and C.B. conducted experiments.

Notes

The authors declare no competing financial interest.

■ ACKNOWLEDGMENTS

These studies were funded by a Wellcome Trust Collaborative Award (201529/Z/16/Z) (A.B.T., A.C., K.J.T., and E.K.). This work was supported by the Intramural Research Program of the NIH, The National Institutes of Diabetes and Digestive and Kidney Diseases (NIDDK), DK075087 (M.J.K.), DK075089 (M.J.K.), U24DK116195 (B.L.R.), UO1MH105892 (B.L.R., J.J., and T.K.) and the NIMH Psychoactive Drug Screening Program (X.P.H., S.S., and B.L.R.). S.J.B. is funded through a Lord Kelvin Adam Smith Fellowship and an MRC project grant (MR/P019366/1). R.H.J.O. is funded through the grant NRSA F31-NS093917, NINDS. We acknowledge the BSU facilities at the Cancer Research U.K. Beatson Institute (C596/A17196) and the Biological Services at the University of Glasgow. We are grateful to Emma Barr for support of the Tobin group.

■ REFERENCES

(1) Lerchner, W., Xiao, C., Nashmi, R., Slimko, E. M., van Trigt, L., Lester, H. A., and Anderson, D. J. (2007) Reversible silencing of neuronal excitability in behaving mice by a genetically targeted, ivermectin-gated Cl- channel. *Neuron 54* (1), 35−49.

(2) Magnus, C. J., Lee, P. H., Atasoy, D., Su, H. H., Looger, L. L., and Sternson, S. M. (2011) Chemical and genetic engineering of selective ion channel-ligand interactions. *Science 333* (6047), 1292−6.

(3) Bishop, A. C., Shah, K., Liu, Y., Witucki, L., Kung, C., and Shokat, K. M. (1998) Design of allele-specific inhibitors to probe protein kinase signaling. *Curr. Biol. 8* (5), 257−66.

(4) Coward, P., Wada, H. G., Falk, M. S., Chan, S. D., Meng, F., Akil, H., and Conklin, B. R. (1998) Controlling signaling with a specifically designed Gi-coupled receptor. *Proc. Natl. Acad. Sci. U. S. A. 95* (1), 352−7.

(5) Westkaemper, R., Hyde, E. G., Choudhary, M. S., Khan, N., Gelbar, E. I., Glennon, R. A., and Roth, B. L. (1999) Engineering in a region of bulk tolerance into the 5-HT2A receptor. *Eur. J. Med. Chem. 34*, 441−447.

(6) Armbruster, B. N., Li, X., Pausch, M. H., Herlitze, S., and Roth, B. L. (2007) Evolving the lock to fit the key to create a family of G protein-coupled receptors potently activated by an inert ligand. *Proc. Natl. Acad. Sci. U. S. A. 104* (12), 5163−8.

(7) Alexander, G. M., Rogan, S. C., Abbas, A. I., Armbruster, B. N., Pei, Y., Allen, J. A., Nonneman, R. J., Hartmann, J., Moy, S. S., Nicolelis, M. A., McNamara, J. O., and Roth, B. L. (2009) Remote control of neuronal activity in transgenic mice expressing evolved G protein-coupled receptors. *Neuron 63* (1), 27−39.

(8) Guettier, J. M., Gautam, D., Scarselli, M., de Azua, I. R., Li, J. H., Rosemond, E., Ma, X., Gonzalez, F. J., Armbruster, B. N., Lu, H., Roth, B. L., and Wess, J. (2009) A chemical-genetic approach to study G protein regulation of beta cell function in vivo. *Proc. Natl. Acad. Sci. U. S. A. 106* (45), 19197−19202.

(9) Nakajima, K. I., and Wess, J. (2012) Design and Functional Characterization of a Novel, Arrestin-Biased Designer G Protein-Coupled Receptor. *Mol. Pharmacol. 82*, 575.

(10) Hu, J., Stern, M., Gimenez, L. E., Wanka, L., Zhu, L., Rossi, M., Meister, J., Inoue, A., Beck-Sickinger, A. G., Gurevich, V. V., and Wess, J. (2016) A G Protein-biased Designer G Protein-coupled Receptor Useful for Studying the Physiological Relevance of Gq/11-dependent Signaling Pathways. *J. Biol. Chem. 291* (15), 7809−20.

(11) Vardy, E., Robinson, J. E., Li, C., Olsen, R. H., DiBerto, J. F., Giguere, P. M., Sassano, F. M., Huang, X. P., Zhu, H., Urban, D. J., White, K. L., Rittiner, J. E., Crowley, N. A., Pleil, K. E., Mazzone, C. M., Mosier, P. D., Song, J., Kash, T. L., Malanga, C. J., Krashes, M. J., and Roth, B. L. (2015) A New DREADD Facilitates the Multiplexed Chemogenetic Interrogation of Behavior. *Neuron 86* (4), 936−46.

(12) Hudson, B. D., Christiansen, E., Tikhonova, I. G., Grundmann, M., Kostenis, E., Adams, D. R., Ulven, T., and Milligan, G. (2012) Chemically engineering ligand selectivity at the free fatty acid receptor 2 based on pharmacological variation between species orthologs. *FASEB J. 26* (12), 4951−65.

(13) Lin, G., McKay, G., and Midha, K. K. (1996) Characterization of metabolites of clozapine N-oxide in the rat by micro-column high performance liquid chromatography/mass spectrometry with electrospray interface. *J. Pharm. Biomed. Anal. 14* (11), 1561−77.

(14) Chang, W. H., Lin, S. K., Lane, H. Y., Wei, F. C., Hu, W. H., Lam, Y. W., and Jann, M. W. (1998) Reversible metabolism of clozapine and clozapine N-oxide in schizophrenic patients. *Prog. Neuro-Psychopharmacol. Biol. Psychiatry 22* (5), 723−39.

(15) Jann, M. W., Lam, Y. W., and Chang, W. H. (1994) Rapid formation of clozapine in guinea-pigs and man following clozapine-N-oxide administration. *Arch. Int. Pharmacodyn. Ther. 328* (2), 243−250.

(16) Raper, J., Morrison, R. D., Daniels, J. S., Howell, L., Bachevalier, J., Wichmann, T., and Galvan, A. (2017) Metabolism and Distribution of Clozapine-N-oxide: Implications for Nonhuman Primate Chemogenetics. *ACS Chem. Neurosci. 8* (7), 1570−1576.

(17) Roth, B. L., Sheffler, D. J., and Kroeze, W. K. (2004) Magic shotguns versus magic bullets: selectively non-selective drugs for mood disorders and schizophrenia. *Nat. Rev. Drug Discovery 3* (4), 353−9.

(18) Yadav, P. N., Abbas, A. I., Farrell, M. S., Setola, V., Sciaky, N., Huang, X. P., Kroeze, W. K., Crawford, L. K., Piel, D. A., Keiser, M. J., Irwin, J. J., Shoichet, B. K., Deneris, E. S., Gingrich, J., Beck, S. G., and Roth, B. L. (2011) The presynaptic component of the serotonergic system is required for clozapine's efficacy. *Neuropsychopharmacology 36* (3), 638−51.

(19) Li, Z., Prus, A. J., Dai, J., and Meltzer, H. Y. (2009) Differential effects of M1 and 5-hydroxytryptamine1A receptors on atypical antipsychotic drug-induced dopamine efflux in the medial prefrontal cortex. *J. Pharmacol. Exp. Ther. 330* (3), 948−55.

(20) Spalding, T. A., Ma, J. N., Ott, T. R., Friberg, M., Bajpai, A., Bradley, S. R., Davis, R. E., Brann, M. R., and Burstein, E. S. (2006) Structural requirements of transmembrane domain 3 for activation by the M1 muscarinic receptor agonists AC-42, AC-260584, clozapine, and N-desmethylclozapine: evidence for three distinct modes of receptor activation. *Mol. Pharmacol. 70* (6), 1974−83.

(21) Sur, C., Mallorga, P. J., Wittmann, M., Jacobson, M. A., Pascarella, D., Williams, J. B., Brandish, P. E., Pettibone, D. J., Scolnick, E. M., and Conn, P. J. (2003) N-desmethylclozapine, an allosteric agonist at muscarinic 1 receptor, potentiates N-methyl-D-aspartate receptor activity. *Proc. Natl. Acad. Sci. U. S. A. 100* (23), 13674−9.

(22) Lameh, J., Burstein, E. S., Taylor, E., Weiner, D. M., Vanover, K. E., and Bonhaus, D. W. (2007) Pharmacology of N-desmethylclozapine. *Pharmacol. Ther. 115* (2), 223−31.

(23) Urban, D. J., and Roth, B. L. (2015) DREADDs (designer receptors exclusively activated by designer drugs): chemogenetic tools with therapeutic utility. *Annu. Rev. Pharmacol. Toxicol. 55*, 399−417.

(24) Burnett, C. J., and Krashes, M. J. (2016) Resolving Behavioral Output via Chemogenetic Designer Receptors Exclusively Activated by Designer Drugs. *J. Neurosci. 36* (36), 9268−82.

DOI: 10.1021/acsptsci.8b00012
ACS Pharmacol. Transl. Sci. 2018, 1, 61−72

(25) Markowitz, J. S., and Patrick, K. S. (1995) Thermal degradation of clozapine-N-oxide to clozapine during gas chromatographic analysis. *J. Chromatogr., Biomed. Appl. 668* (1), 171−4.
(26) Roth, B. L. (2016) DREADDs for Neuroscientists. *Neuron 89* (4), 683−94.
(27) MacLaren, D. A., Browne, R. W., Shaw, J. K., Krishnan Radhakrishnan, S., Khare, P., Espana, R. A., and Clark, S. D. (2016) Clozapine N-Oxide Administration Produces Behavioral Effects in Long-Evans Rats: Implications for Designing DREADD Experiments. *eNeuro 3* (5), 0219-16.2016.
(28) Gomez, J. L., Bonaventura, J., Lesniak, W., Mathews, W. B., Sysa-Shah, P., Rodriguez, L. A., Ellis, R. J., Richie, C. T., Harvey, B. K., Dannals, R. F., Pomper, M. G., Bonci, A., and Michaelides, M. (2017) Chemogenetics revealed: DREADD occupancy and activation via converted clozapine. *Science 357* (6350), 503−507.
(29) Hellman, K., Aadal Nielsen, P., Ek, F., and Olsson, R. (2016) An ex Vivo Model for Evaluating Blood-Brain Barrier Permeability, Efflux, and Drug Metabolism. *ACS Chem. Neurosci. 7* (5), 668−80.
(30) Chen, X., Choo, H., Huang, X. P., Yang, X., Stone, O., Roth, B. L., and Jin, J. (2015) The first structure-activity relationship studies for designer receptors exclusively activated by designer drugs. *ACS Chem. Neurosci. 6* (3), 476−84.
(31) Bradley, S. J., Bourgognon, J. M., Sanger, H. E., Verity, N., Mogg, A. J., White, D. J., Butcher, A. J., Moreno, J. A., Molloy, C., Macedo-Hatch, T., Edwards, J. M., Wess, J., Pawlak, R., Read, D. J., Sexton, P. M., Broad, L. M., Steinert, J. R., Mallucci, G. R., Christopoulos, A., Felder, C. C., and Tobin, A. B. (2017) M1 muscarinic allosteric modulators slow prion neurodegeneration and restore memory loss. *J. Clin. Invest. 127* (2), 487−499.
(32) Conn, P. J., Christopoulos, A., and Lindsley, C. W. (2009) Allosteric modulators of GPCRs: a novel approach for the treatment of CNS disorders. *Nat. Rev. Drug Discovery 8* (1), 41−54.
(33) Wess, J., Eglen, R. M., and Gautam, D. (2007) Muscarinic acetylcholine receptors: mutant mice provide new insights for drug development. *Nat. Rev. Drug Discovery 6* (9), 721−33.
(34) Motulsky, H., and Christopoulos, A. (2004) *Fitting Models to Biological Data Using Linear and Nonlinear Regression: A Practical Guide to Curve Fitting*, Oxford University Press.
(35) Yung-Chi, C., and Prusoff, W. H. (1973) Relationship between the inhibition constant (Ki) and the concentration of inhibitor which causes 50% inhibition (I50) of an enzymatic reaction. *Biochem. Pharmacol. 22* (23), 3099−3108.
(36) Christopoulos, A. (1998) Assessing the distribution of parameters in models of ligand−receptor interaction: to log or not to log. *Trends Pharmacol. Sci. 19* (9), 351−357.
(37) Kroeze, W. K., Sassano, M. F., Huang, X. P., Lansu, K., McCorvy, J. D., Giguere, P. M., Sciaky, N., and Roth, B. L. (2015) PRESTO-Tango as an open-source resource for interrogation of the druggable human GPCRome. *Nat. Struct. Mol. Biol. 22* (5), 362−9.
(38) Betley, J. N., Xu, S., Cao, Z. F. H., Gong, R., Magnus, C. J., Yu, Y., and Sternson, S. M. (2015) Neurons for hunger and thirst transmit a negative-valence teaching signal. *Nature 521* (7551), 180−185.
(39) Burnett, C. J., Li, C., Webber, E., Tsaousidou, E., Xue, S. Y., Bruning, J. C., and Krashes, M. J. (2016) Hunger-Driven Motivational State Competition. *Neuron 92* (1), 187−201.
(40) Chen, Y., Lin, Y. C., Kuo, T. W., and Knight, Z. A. (2015) Sensory detection of food rapidly modulates arcuate feeding circuits. *Cell 160* (5), 829−41.
(41) Mandelblat-Cerf, Y., Ramesh, R. N., Burgess, C. R., Patella, P., Yang, Z., Lowell, B. B., and Andermann, M. L. (2015) Arcuate hypothalamic AgRP and putative POMC neurons show opposite changes in spiking across multiple timescales. *eLife 4*, 07122.
(42) Krashes, M. J., Koda, S., Ye, C., Rogan, S. C., Adams, A. C., Cusher, D. S., Maratos-Flier, E., Roth, B. L., and Lowell, B. B. (2011) Rapid, reversible activation of AgRP neurons drives feeding behavior in mice. *J. Clin. Invest. 121* (4), 1424−8.
(43) Aponte, Y., Atasoy, D., and Sternson, S. M. (2011) AGRP neurons are sufficient to orchestrate feeding behavior rapidly and without training. *Nat. Neurosci. 14* (3), 351−5.
(44) Gropp, E., Shanabrough, M., Borok, E., Xu, A. W., Janoschek, R., Buch, T., Plum, L., Balthasar, N., Hampel, B., Waisman, A., Barsh, G. S., Horvath, T. L., and Bruning, J. C. (2005) Agouti-related peptide-expressing neurons are mandatory for feeding. *Nat. Neurosci. 8* (10), 1289−91.
(45) Luquet, S., Perez, F. A., Hnasko, T. S., and Palmiter, R. D. (2005) NPY/AgRP neurons are essential for feeding in adult mice but can be ablated in neonates. *Science 310* (5748), 683−685.
(46) Krashes, M. J., Shah, B. P., Koda, S., and Lowell, B. B. (2013) Rapid versus delayed stimulation of feeding by the endogenously released AgRP neuron mediators GABA, NPY, and AgRP. *Cell Metab. 18* (4), 588−95.
(47) Atasoy, D., Betley, J. N., Su, H. H., and Sternson, S. M. (2012) Deconstruction of a neural circuit for hunger. *Nature 488* (7410), 172−7.
(48) Garfield, A. S., Li, C., Madara, J. C., Shah, B. P., Webber, E., Steger, J. S., Campbell, J. N., Gavrilova, O., Lee, C. E., Olson, D. P., Elmquist, J. K., Tannous, B. A., Krashes, M. J., and Lowell, B. B. (2015) A neural basis for melanocortin-4 receptor-regulated appetite. *Nat. Neurosci. 18* (6), 863−71.
(49) Holder, J. L., Jr., Zhang, L., Kublaoui, B. M., DiLeone, R. J., Oz, O. K., Bair, C. H., Lee, Y. H., and Zinn, A. R. (2004) Sim1 gene dosage modulates the homeostatic feeding response to increased dietary fat in mice. *Am. J. Physiol Endocrinol Metab 287* (1), E105−13.
(50) Xi, D., Gandhi, N., Lai, M., and Kublaoui, B. M. (2012) Ablation of Sim1 neurons causes obesity through hyperphagia and reduced energy expenditure. *PLoS One 7* (4), e36453.
(51) Vardy, E., Robinson, J. E., Li, C., Olsen, R. H. J., DiBerto, J. F., Giguere, P. M., Sassano, F. M., Huang, X. P., Zhu, H., Urban, D. J., White, K. L., Rittiner, J. E., Crowley, N. A., Pleil, K. E., Mazzone, C. M., Mosier, P. D., Song, J., Kash, T. L., Malanga, C. J., Krashes, M. J., and Roth, B. L. (2015) A New DREADD Facilitates the Multiplexed Chemogenetic Interrogation of Behavior. *Neuron 86* (4), 936−946.
(52) Stachniak, T. J., Ghosh, A., and Sternson, S. M. (2014) Chemogenetic synaptic silencing of neural circuits localizes a hypothalamus−>midbrain pathway for feeding behavior. *Neuron 82* (4), 797−808.
(53) Shi, Z., Madden, C. J., and Brooks, V. L. (2017) Arcuate neuropeptide Y inhibits sympathetic nerve activity via multiple neuropathways. *J. Clin. Invest. 127* (7), 2868−2880.
(54) Krashes, M., Koda, S., Ye, C., Rogan, S. C., Adams, A., Cusher, D. S., Maratos-Flier, E., Roth, B. L., and Lowell, B. (2011) Rapid, Reversible Activation of AgRP Neurons Drives Feeding Behavior. *J. Clin. Invest. 121*, 1424−1428.
(55) Besnard, J., Ruda, G. F., Setola, V., Abecassis, K., Rodriguiz, R. M., Huang, X.-P., Norval, S., Sassano, M. F., Shin, A. I., and Webster, L. A. (2012) Automated design of ligands to polypharmacological profiles. *Nature 492*, 215−220.

DOI: 10.1021/acsptsci.8b00012
ACS Pharmacol. Transl. Sci. 2018, 1, 61−72